Missouri University of Science and Technology
Scholars' Mine

Electrical and Computer Engineering Faculty Research & Creative Works

Electrical and Computer Engineering

01 Jan 2022

Robust Modifications to Model Reference Adaptive Control for Reference Voltage Tracking in a Dual Active Bridge Dc-Dc Converter

Kartikeya J.P. Veeramraju

Alvaro Cardoza

Jagannathan Sarangapani
Missouri University of Science and Technology, sarangap@mst.edu

Jonathan W. Kimball
Missouri University of Science and Technology, kimballjw@mst.edu

Follow this and additional works at: https://scholarsmine.mst.edu/ele_comeng_facwork

 Part of the Electrical and Computer Engineering Commons

Recommended Citation

K. J. Veeramraju et al., "Robust Modifications to Model Reference Adaptive Control for Reference Voltage Tracking in a Dual Active Bridge Dc-Dc Converter," *2022 IEEE Energy Conversion Congress and Exposition, ECCE 2022*, Institute of Electrical and Electronics Engineers, Jan 2022.
The definitive version is available at https://doi.org/10.1109/ECCE50734.2022.9947779

This Article - Conference proceedings is brought to you for free and open access by Scholars' Mine. It has been accepted for inclusion in Electrical and Computer Engineering Faculty Research & Creative Works by an authorized administrator of Scholars' Mine. This work is protected by U. S. Copyright Law. Unauthorized use including reproduction for redistribution requires the permission of the copyright holder. For more information, please contact scholarsmine@mst.edu.

Robust Modifications to Model Reference Adaptive Control for Reference Voltage Tracking in a Dual Active Bridge dc-dc Converter

Kartikeya JP Veeramraju
Department of Electrical and Computer Engineering
Missouri University of Science and Technology
Rolla, MO USA
kvkhh@mst.edu

Alvaro Cardoza
Department of Electrical and Computer Engineering
Missouri University of Science and Technology
Rolla, MO USA
acbk4@mst.edu

Jagannathan Sarangapani
Department of Electrical and Computer Engineering
Missouri University of Science and Technology
Rolla, MO USA
sarangap@mst,edu

Jonathan W Kimball
Department of Electrical and Computer Engineering
Missouri University of Science and Technology
Rolla, MO USA
kimballjw@mst.edu

2022 IEEE Energy Conversion Congress and Exposition (ECCE) | 978-1-7281-9387-8/22/$31.00 ©2022 IEEE | DOI: 10.1109/ECCE50734.2022.9947779

***Abstract*—Model Reference Adaptive Control (MRAC) is useful for achieving a desired dynamic response with no prior knowledge of system parameters. Traditional MRAC is sensitive to noise in the state variables, leading to adaptation parametric drift. The drift in parameters, if left unchecked, leads to loss of closed loop stability. In power electronic systems, the ripple in the output voltage serves as a bounded noise, which leads to MRAC instability. This drift phenomenon is observed through the simulation and hardware experimentation of a Dual Active Bridge (DAB) converter, and mitigated using deadzone modification and σ modification approaches. These two methods are then compared to evaluate their respective strengths and weaknesses for practical hardware implementation of power electronics using MRAC.**

***Index Terms*—Dual Active Bridge converter, Robust Adaptive Control, Model Reference Adaptive Control**

I. Introduction

The Dual Active Bridge (DAB) is a dc-dc converter suitable for high power bidirectional power flow control with galvanic isolation [1]. DABs are suitable for many applications such as microgrids [2]–[4], solid state transformers [5]–[8], aerospace power systems [9], [10]. A functional schematic of the DAB is shown in Fig. 1. Due to this wide range of application space of the DAB, many methods of switching the converter are proposed [1], namely single phase shift modulation (SPS), double phase shift modulation and triple phase shift modulation. In this article, the SPS strategy is used for switching the DAB.

Many control strategies have been proposed for controlling the DAB such as conventional linear control techniques [11], [12]. However such control techniques need parametric values in the converter, which may or may not be accurately obtainable. This will lead to unsatisfactory dynamic performance.

Adaptive control techniques, on the other hand, relax the necessity to know the parameters of the system prior to controller

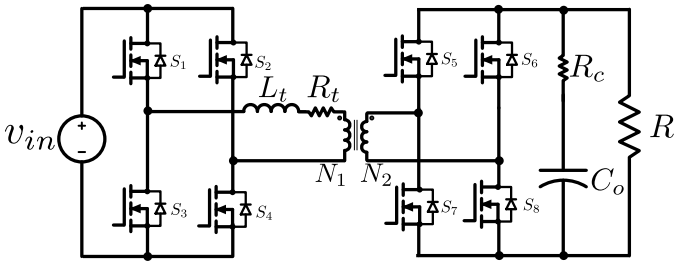

Fig. 1: Schematic of a dc-dc DAB converter

implementation, making them suitable for scenarios where the dynamic behavior is to be tightly controlled.Model Reference Adaptive Control (MRAC) is an effective control technique as it adjusts the system response based on continuously adjusting for parametric variations. A block diagrammatic representation of MRAC is shown in Fig. 2. The nature of plant dynamics are crucial for MRAC implementation. Once the plant's dynamics are modeled properly, MRAC ensures asymptotic stability of the tracking error. But when a plant is modeled for control, only a certain level of abstraction is captured in the mathematical model. These unmodeled plant dynamics and behaviors, lead to classical MRAC adaptation parameter instability. This behavior is known as parametric drift [13]–[15]. If the drift is unchecked, the closed loop system stability cannot be guaranteed. Robust modifications [13] are therefore proposed to counteract these drift induced effects that lead to a stable closed loop system.

Classical MRAC is formulated and simulated under ideal conditions in [16]. Classical MRAC suffers from parametric drift effects as a DAB's output voltage contains a bounded ripple. The parametric drift is found to adversely affect the sta-

978-1-7281-9387-8/22/$31.00 ©2022 IEEE

Authorized licensed use limited to: Missouri University of Science and Technology. Downloaded on February 17,2023 at 18:46:27 UTC from IEEE Xplore. Restrictions apply.

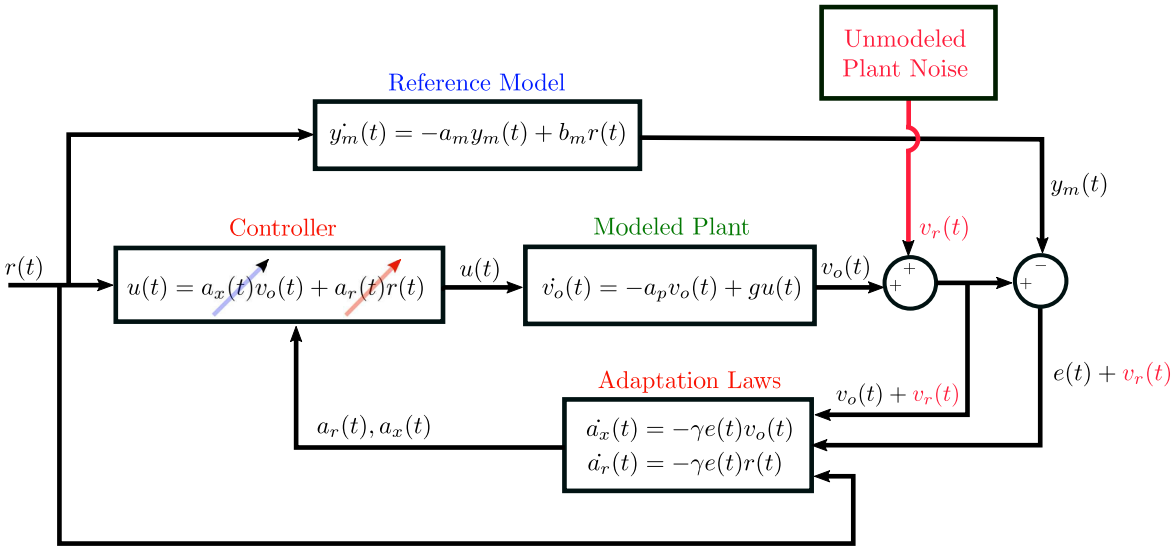

Fig. 2: Block diagram of classical MRAC with unmodeled plant noise

bility of the system when faster response rates are demanded out of the controller. The main contributions of this article in this regards include:

1) DAB hardware implementation to prove the parametric drift effects in classical MRAC
2) Adaptation law modification using the dead-zone technique to counteract parametric drift and validation using hardware implementation to show alleviation of parametric drift

In this article, the dynamic model of the DAB converter is first modeled in Section II. Then the various MRAC techniques are discussed in Section III. Following this, the MRAC schemes discussed earlier are implemented on hardware in Section IV, followed by conclusions in Section V

II. DAB Converter Model

The schematic of the DAB is shown in Fig. 1. The dynamic equations for the DAB are written as

$$L_t \frac{di_t(t)}{dt} = v_s q_1(t) - R_o i_t(t) - \frac{N_1}{N_2}\frac{R}{R+R_c} q_2(t) v_c(t) \quad (1)$$

$$C_o \frac{dv_c(t)}{dt} = \frac{N_1}{N_2}\frac{R}{R+R_c} q_2(t) i_t(t) - \frac{1}{R+R_c} v_c(t), \quad (2)$$

where the two differential equations pertain to the leakage inductance L_t, the filter capacitance C_o, and the equivalent series resistances of C_o and L_t, which are denoted by R_c, and R_t, respectively. The load is characterized as a pure resistance R connected across the capacitor C_o. The transformer's secondary to primary turns ratio is $N_2 : N_1$. The two bridges of the DAB are modulated by switching functions $q_1(t)$ and $q_2(t)$. The inductor current and capacitor voltage states are represented by $i_t(t)$ and $v_c(t)$, respectively. R_o is an intermediate-term given by

$$R_o = \frac{R_t R + R_t R_c + R R_c \frac{N_1^2}{N_2^2}}{R + R_c}. \quad (3)$$

The reduced-order average model (ROAM) [16] for the output voltage dynamics $\dot{v_o}(t)$ of the DAB converter from the Generalized Average Model (GAM) [17] is derived to be

$$\dot{v_o}(t) = f(v_o(t)) + gu \quad (4)$$

with

$$f(v_o) = -\frac{v_o(t)}{(R+R_c)C_o} = -a_p v_o(t) \quad (5)$$

$$g = \frac{8}{\pi^2}\frac{R}{(R+R_c)C_o}\frac{N_2 V_{in}}{N_1|Z|} \quad (6)$$

$$|Z| = \sqrt{R_o^2 + (\omega L_t)^2}, \quad (7)$$

where $u = \sin(\phi)$ with ϕ being the actual phase shift needed between primary and secondary bridges for power flow control. With the ROAM formulated, the MRAC control can be derived in the subsequent sections.

III. MRAC formulation and robust modifications with simulations

In this section, the model (4) will be used to formulate a direct MRAC controller for output voltage tracking applications.

A. Classical MRAC

The functional block diagram of MRAC is shown in Fig. 2, which shows that classical MRAC closed loop system has four parts: the control law, the plant, the reference model, and the adaptation laws. The necessary condition for the stability of the closed-loop system is that the reference model be stable. As the DAB model in (4) is a first-order system, the reference model must also be a first-order system. The reference model is therefore

$$\dot{y}_m = -a_m y_m + b_m r(t), \quad (8)$$

Authorized licensed use limited to: Missouri University of Science and Technology. Downloaded on February 17,2023 at 18:46:27 UTC from IEEE Xplore. Restrictions apply.

where a_m and b_m are the reference model parameters, y_m is the state of the reference model that is used for error generation, and $r(t)$ is the reference value fed to the plant that the DAB must ultimately track. The control law is defined as

$$u \triangleq a_r(t)r(t) + a_x(t)x(t) \tag{9}$$

where $a_r(t)$, $a_x(t)$ are estimates of the control parameters for compensating the unknowns of the system. The DAB parameters are all assumed to be unknown. That is, the value of C, R, R_c, R_t, v_{in}, $|Z|$, N_2, and N_1 are unknown, which makes a_p, and g unknown quantities. However, the sign of g is positive as all passive components are known to have a positive real value and the input voltage is also positive. The error $e(t) = v_o(t) - y_m(t)$ of the model produces error dynamics of

$$\dot{e}(t) = -a_m e(t) + g\tilde{a}_x(t)x(t) + g\tilde{a}_r(t)r(t), \tag{10}$$

where $\tilde{a}_r(t) = a_r(t) - b_m/g$ and $\tilde{a}_x(t) = a_x(t) - (a_p - a_m)/g$. The model matching condition is satisfied when $\tilde{a}_r(t)$, $\tilde{a}_x(t)$ are both zero. Now a Lyapunov candidate can be chosen to formulate the adaptive control laws. The chosen candidate Lyapunov function is

$$V = \frac{e^2}{2} + \frac{|g|}{2\gamma}(\tilde{a}_x^2 + \tilde{a}_r^2), \tag{11}$$

where γ is a positive constant that serves as a tuning parameter to control the rate of adaptation. The proof of the Lyapunov stability is given below.

Proof:

$$\begin{aligned}
\dot{V} &= e(t)\dot{e}(t) + \frac{|g|}{\gamma}(\tilde{a}_x(t)\dot{\tilde{a}}_x(t) + \tilde{a}_r(t)\dot{\tilde{a}}_r(t)) \\
&= e(t)(a_m e(t) + g\tilde{a}_x(t)x(t) + g\tilde{a}_r(t)r(t)) \\
&+ \frac{|g|}{\gamma}(\tilde{a}_x(t)\dot{\tilde{a}}_x(t) + \tilde{a}_r(t)\dot{\tilde{a}}_r(t)) \\
&= -a_m e^2(t) + \tilde{a}_x(t)\left(ge(t)x_p(t) + \frac{|g|}{\gamma}\dot{\tilde{a}}_x(t)\right) \\
&+ \tilde{a}_r(t)\left(ge(t)r(t) + \frac{|g|}{\gamma}\dot{\tilde{a}}_r(t)\right) \\
\dot{V} &\leq 0
\end{aligned}$$

In order to maintain $\dot{V} \leq 0$, the last two terms can be canceled out to zero to get a negative semi-definite result for $\dot{V}$. Realizing that $g = |g|\text{sgn}(g)$, the second term is written as

$$e(t)|g|\text{sgn}(g)x(t) = -\frac{|g|}{\gamma}\dot{\tilde{a}}_x \tag{12}$$

and the last term as

$$e(t)|g|\text{sgn}(g)r(t) = -\frac{|g|}{\gamma}\dot{\tilde{a}}_r. \tag{13}$$

Therefore, two adaptation laws are obtained:

$$\dot{\tilde{a}}_x = -\gamma\text{sgn}(g)e(t)v_o(t) \tag{14}$$

$$\dot{\tilde{a}}_r = -\gamma\text{sgn}(g)e(t)r(t) \tag{15}$$

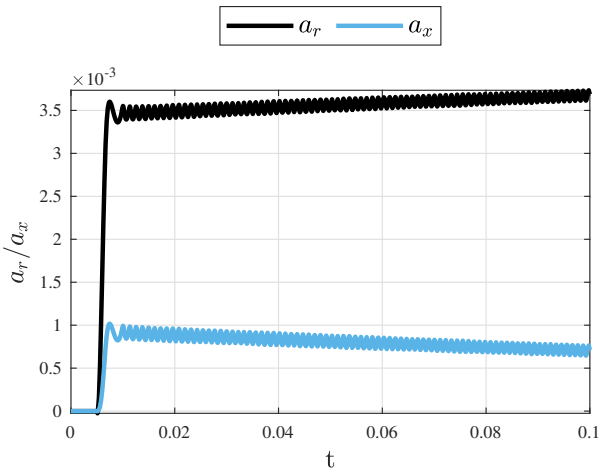

Fig. 3: Parametric drift in classical MRAC simulation

By Barbalat's lemma, one can show that $e(t)$ converges asymptotically to zero. However, *the convergence of* $\tilde{a}_r(t)$ *and* $\tilde{a}_x(t)$ *cannot be guaranteed unless the Persistency of Excitation (PE) condition is guaranteed* [13]. The ramifications of the parameter estimate not being bounded will be discussed in the next section, and a robust modification will make relaxations to the PE conditions to the existing adaptive control laws.

B. MRAC performance under bounded noise

If a bounded noise is present on the plant (as seen in Fig. 2) and was initially unmodeled, the plant equation is rewritten as

$$\dot{v_o}(t) = -a_p v_o(t) + gu(t) + v_r(t), \tag{16}$$

where $v_r(t)$ is the unmodeled bounded noise in the plant. This changes the error dynamics to

$$\dot{e}(t) = -a_m e(t) + g\tilde{a}_x(t)x(t) + g\tilde{a}_r(t)r(t) + v_r(t), \tag{17}$$

which in turn leads the derivative of the Lyapunov to be

$$\begin{aligned}
\dot{V} &= -a_m e^2(t) + \tilde{a}_x(t)\left(ge(t)x_p(t) + \frac{|g|}{\gamma}\dot{\tilde{a}}_x(t)\right) \\
&+ \tilde{a}_r(t)\left(ge(t)r(t) + \frac{|g|}{\gamma}\dot{\tilde{a}}_r(t)\right) + e(t)v_r(t)
\end{aligned} \tag{18}$$

Due to the negative semidefiniteness, the stability of $e(t)$ can be shown, but the stability of adaptation parameters cannot be shown. This means that the adaptation parameters can reach high values if left unchecked, and create a control term u that the actuator system may not be able to generate, ultimately leading to instability.

C. Robust Adaptive Control

In order to prevent this unwanted behavior, robust adaptive control techniques can be used. The techniques relax the persistency of excitation requirements to guarantee parametric convergence. To this effect, two methods will be discussed: deadzone modification and σ modification.

Authorized licensed use limited to: Missouri University of Science and Technology. Downloaded on February 17,2023 at 18:46:27 UTC from IEEE Xplore. Restrictions apply.

TABLE I: Operation Parameters

Parameter	f_{sw}	V_{in}	V_o	C_o	R_c	N_2/N_1	R_t	L_{lk}	R
Value	80 kHz	14 V	20 V	40 µF	3.3 mΩ	1.11	49.6 mΩ	3.5 µH	33.33 Ω

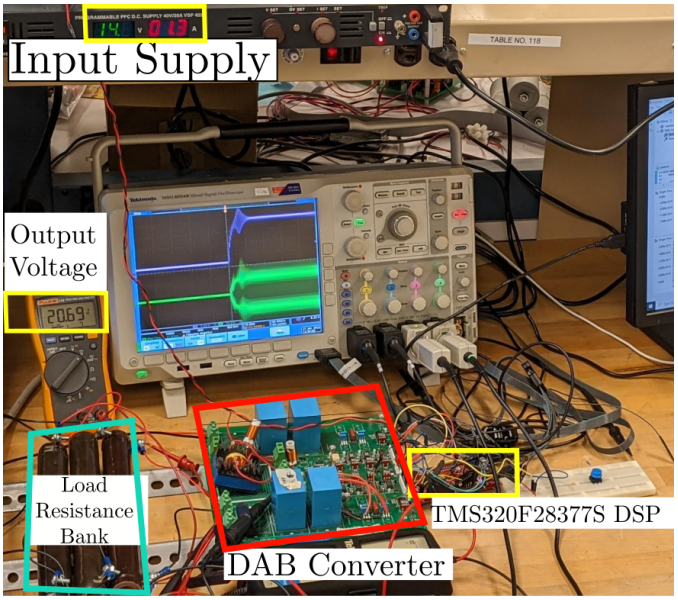

Fig. 4: Hardware setup for DAB converter running on classical MRAC

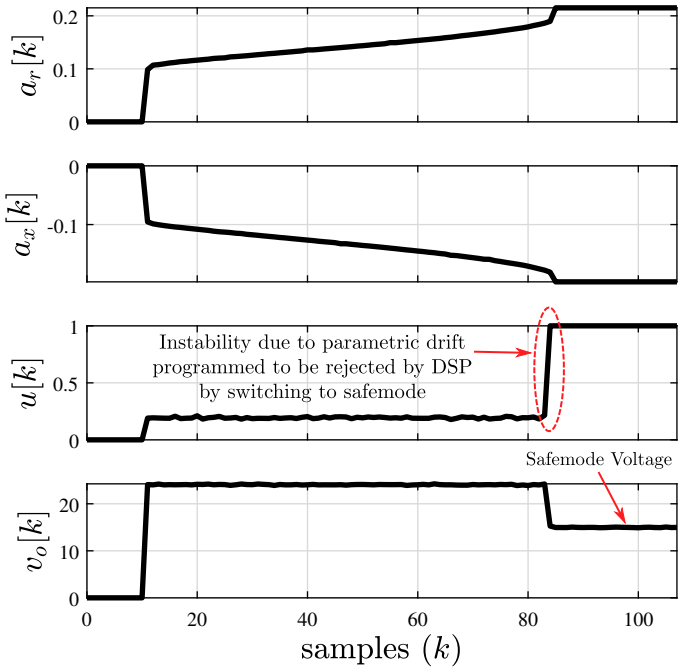

Fig. 5: Instability in classical MRAC, for $\gamma = 2.6, v_{o\,\text{ref}} = 24\,\text{V}$ observed on hardware experimentation. The parametric drift causes sudden onset of very high control effort.

1) Deadzone Modification: A trial and error based method like the deadzone modification [13]–[15] technique modifies the adaptive laws to

$$\frac{d}{dt}a_r(t) = \begin{cases} -\text{sgn}(g)\gamma e(t) r(t) & \|e\| > e_{\text{bound}} \\ 0 & \|e\| \leq e_{\text{bound}} \end{cases} \tag{19}$$

$$\frac{d}{dt}a_x(t) = \begin{cases} -\text{sgn}(g)\gamma e(t) v_o(t) & \|e\| > e_{\text{bound}} \\ 0 & \|e\| \leq e_{\text{bound}} \end{cases}, \tag{20}$$

where e_{bound} is the error bound beyond which the adaptation law is to be applied. The disadvantage of using deadzone modification is the setting of e_{bound}. However, *as the main source of bounded unmodeled noise in many standard power electronic converters is due to the output voltage ripple, a power electronic designer can easily determine the value of the ripple via simulations and set this limit in hardware*. This makes deadzone modification highly suitable for power electronic converter control.

2) σ Modification: Although the error bound is useful for practical implementation, the output voltage ripple is sensitive to load current changes, which is common in a power electronic converter. Using a single e_{bound} value for all loading levels on the converter is not feasible, as the ripple value changes. Therefore, a more robust method like the well known σ modification method [13]–[15] is useful. In this scheme, the adaptation laws are modified as

$$\frac{d}{dt}a_r(t) = -\gamma(e(t)r(t) + \sigma a_r(t)) \tag{21}$$

$$\frac{d}{dt}a_x(t) = -\gamma(e(t)x(t) + \sigma a_x(t)), \tag{22}$$

where $\sigma > 0$ is the modification parameter. The modification term introduces a constant damping into the adaptive law, thereby providing a mechanism to bound the adaptive parameter. This control makes the system Stable in the Sense of Lyapunov (SISL), and therefore does not guarantee asymptotic convergence on the tracking error. However, the trial and error method of selecting the e_{bound} is relaxed.

D. Simulation verification

Upon simulation of the DAB converter on PLECS® using classical MRAC, the voltage ripple on the output capacitor is found to serve as the bounded noise v_r, thereby causing the adaptation parameters to drift as shown in Fig. 3.

IV. Hardware Results

In this section, the hardware implementation of the control schemes discussed in Section III will be presented. For the purpose of implementation, a hardware model of the DAB

Authorized licensed use limited to: Missouri University of Science and Technology. Downloaded on February 17,2023 at 18:46:27 UTC from IEEE Xplore. Restrictions apply.

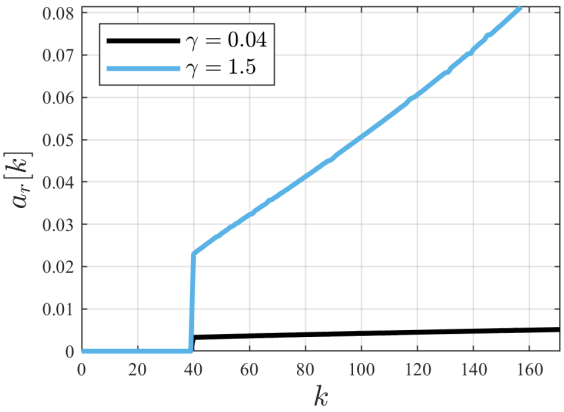

(a) Classical MRAC run for two sets of γ, a_m, and b_m values

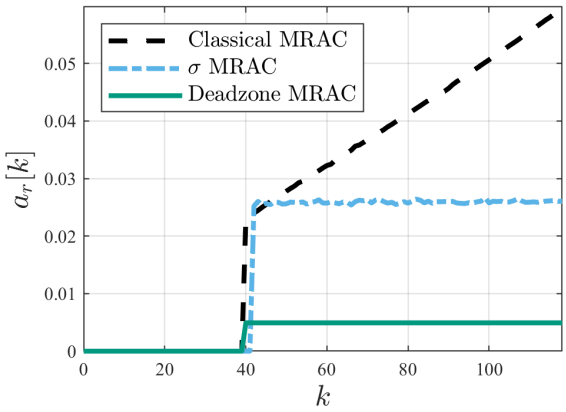

(b) Classical MRAC vs Deadzone vs σ MRAC for $\gamma = 1.5$, $a_m = b_m = 1000$

Fig. 6: Parametric drift for $a_r[k]$ observed due to bounded noise in **hardware tests**. The samples k are acquired in debug mode at 100 Hz sampling rate

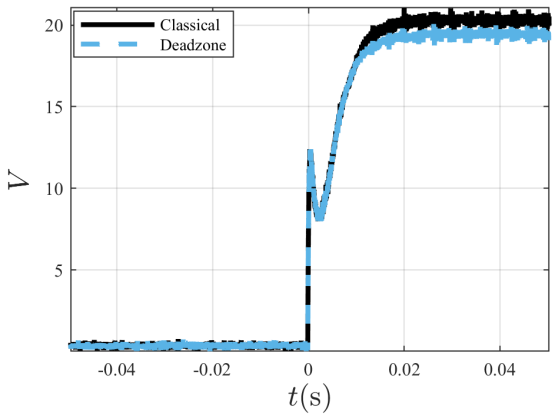

(a) $\gamma = 0.04$, $a_m = b_m = 500$

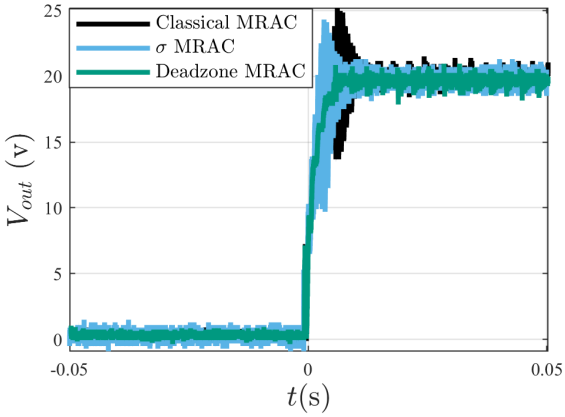

(b) $\gamma = 1.5$, $a_m = b_m = 1000$

Fig. 7: Output voltage of hardware DAB during controller startup for MRAC run with and without deadzone modification for different reference model parameters

with the parameters in Table I is constructed as shown in Fig. 4. For the purpose of control, a C2000 class DSP running a TMS320F28377S on a Launchpad was selected.

A. Implementation note

The reference model (8) was approximated by a Zero Order Hold (ZOH) approximation using the `c2d` function on MATLAB®, while the adaptation laws were discretized using backward Euler method. For example, the discrete adaptive laws for their continuous time counterparts in (14), (15) are given by

$$a_r[k+1] = a_r[k] - \gamma T_s e_m[k] r[k] \tag{23}$$

$$a_x[k+1] = a_x[k] - \gamma T_s e_m[k] v_o[k] \tag{24}$$

for a sampling interval of T_s, which is set to the switching frequency of the DAB for all MRAC implementations in this paper.

The control signal u in (9) is converted to phase angle difference between the H bridges by applying $\phi = \sin^{-1}(u)$ and is passed to the C2000's enhanced Pulse Width Modulation (ePWMx) block for deployment within each Interrupt Service Routine (ISR) cycle.

B. Classical MRAC

The tests were first performed using classical MRAC (14), (15) and the parametric drift described in the earlier section was observed by extracting the parametric update laws ($a_r[k]$,$a_x[k]$) in the Code Composer Studio's debug mode. Figure 6a shows the parametric drift for the two adaptation gain γ parameters and how a higher gain leads to a faster drift in $a_r[k]$ parameter updates, for sample number k. The purpose of γ is to make the adaptation process faster so that the faster referencing tracking is possible.

When implemented on classical MRAC, the controller was found to initially track the reference satisfactorily and the output voltage was found to be stable at the requested setpoint of 24 V, as shown in Fig. 5. However, the adaptation parameters were found to be drifting. When the a_r, a_x parameters drifted

Authorized licensed use limited to: Missouri University of Science and Technology. Downloaded on February 17,2023 at 18:46:27 UTC from IEEE Xplore. Restrictions apply.

significantly, the closed loop system became unstable due to large control inputs that the controller was giving the plant. The time of initiation of system instability depends on the value of γ. Higher values of γ led to the faster instability in the system.

Therefore, the classical MRAC formulation is unsuitable for practical hardware implementation as the PE condition isn't satisfied and the noise drives the parametric estimates high causing controller saturation.

C. Deadzone MRAC

The deadzone modified adaptation laws are run for $\gamma = 1.5$, in Figure 6b which shows how the controller arrests the adaptations when the output reaches the deadzone. Therefore, the deadzone provides robustness against process and sensor noise, which was not previously considered in classical MRAC.

The startup transients with MRAC are shown in Figure. 7a and Figure. 7b. In each plot, the output voltage obtained from classical MRAC is compared with the output voltage obtained with deadzone modification. The deadzone MRAC introduces a steady state error when $e(t)$ reaches the bound.

D. σ Modified MRAC

In the final test for σ modified MRAC, a deadzone is no longer required as explained in Section III. The adaptation parameters settle and do not drift under the bounded noise from voltage ripple effects. The value of σ is selected to be 0.05. The adaptation laws in discrete domain are given by

$$a_r[k+1] = a_r[k] - \gamma T_s e_m[k] r[k] - \gamma \sigma a_r[k] \tag{25}$$

$$a_x[k+1] = a_x[k] - \gamma T_s e_m[k] v_o[k] - \gamma \sigma a_x[k] \tag{26}$$

Due to SISL, the error term does not go to zero, thereby leading to a steady state error in tracking. However, the reference model tracking is satisfactory and the adaptation parameters are bounded and stable, even without the knowledge of error bounds.

V. Conclusions

In this paper, DAB hardware experiments for classical MRAC are presented and their shortcomings are outlined. A reduced-order average model of the DAB's output voltage dynamics are discussed for use with MRAC. The output voltage ripple behaves as a bounded noise to the classical MRAC and leads to parametric drift, which if left unchecked, leads to controller instability. The deadzone modification and σ modification methods are shown to remove the issue of parametric drift under the presence of voltage ripple, thereby leading to robust closed loop control.

Acknowledgment

This material is based upon work supported by the Department of Energy Vehicle Technologies Office under Award Number DE-EE0008449. This report was prepared as an account of work sponsored by an agency of the United States Government. Neither the United States Government nor any agency thereof, nor any of their employees, makes any warranty, express or implied, or assumes any legal liability or responsibility for the accuracy, completeness, or usefulness of any information, apparatus, product, or process disclosed, or represents that its use would not infringe privately owned rights. Reference herein to any specific commercial product, process, or service by trade name, trademark, manufacturer, or otherwise does not necessarily constitute or imply its endorsement, recommendation, or favoring by the United States Government or any agency thereof. The views and opinions of authors expressed herein do not necessarily state or reflect those of the United States Government or any agency thereof.

References

[1] A. K. Jain and R. Ayyanar, "Pwm control of dual active bridge: Comprehensive analysis and experimental verification," *IEEE Transactions on Power Electronics*, vol. 26, no. 4, pp. 1215–1227, 2011.

[2] Q. Ye, R. Mo, and H. Li, "Low-frequency resonance suppression of a dual-active-bridge dc/dc converter enabled dc microgrid," *IEEE Journal of Emerging and Selected Topics in Power Electronics*, vol. 5, no. 3, pp. 982–994, 2017.

[3] M. Cupelli, S. K. Gurumurthy, S. K. Bhanderi, Z. Yang, P. Joebges, A. Monti, and R. W. De Doncker, "Port controlled hamiltonian modeling and ida-pbc control of dual active bridge converters for dc microgrids," *IEEE Transactions on Industrial Electronics*, vol. 66, no. 11, pp. 9065–9075, 2019.

[4] L. Chen, F. Gao, K. Shen, Z. Wang, L. Tarisciotti, P. Wheeler, and T. Dragičević, "Predictive control based dc microgrid stabilization with the dual active bridge converter," *IEEE Transactions on Industrial Electronics*, vol. 67, no. 10, pp. 8944–8956, 2020.

[5] K. J. Veeramraju, A. Sharma, and J. W. Kimball, "A comprehensive analysis on complex power flow mechanism in an ac-ac dual active bridge," in *2022 IEEE Power and Energy Conference at Illinois (PECI)*, 2022, pp. 1–6.

[6] H. Qin and J. W. Kimball, "Solid-state transformer architecture using ac–ac dual-active-bridge converter," *IEEE Transactions on Industrial Electronics*, vol. 60, no. 9, pp. 3720–3730, 2013.

[7] A. Sharma, K. J. Veeramraju, and J. W. Kimball, "Power flow control of a single-stage ac-ac solid-state transformer for ac distribution system," in *2022 IEEE Power and Energy Conference at Illinois (PECI)*, 2022, pp. 1–6.

[8] D. Gonzalez-Agudelo, A. Escobar-Mejía, and H. Ramirez-Murrillo, "Dynamic model of a dual active bridge suitable for solid state transformers," in *2016 13th International Conference on Power Electronics (CIEP)*, 2016, pp. 350–355.

[9] G. Buticchi, D. Barater, L. F. Costa, and M. Liserre, "A pv-inspired low-common-mode dual-active-bridge converter for aerospace applications," *IEEE Transactions on Power Electronics*, vol. 33, no. 12, pp. 10 467–10 477, 2018.

[10] R. T. Naayagi, A. J. Forsyth, and R. Shuttleworth, "Performance analysis of extended phase-shift control of dab dc-dc converter for aerospace energy storage system," in *2015 IEEE 11th International Conference on Power Electronics and Drive Systems*, 2015, pp. 514–517.

[11] A. Bhattacharjee and I. Batarseh, "Improved response of closed loop dual active bridge converter using combined feedback and feed-forward control," in *2019 IEEE Conference on Power Electronics and Renewable Energy (CPERE)*, 2019, pp. 425–430.

[12] S. Shao, L. Chen, Z. Shan, F. Gao, H. Chen, D. Sha, and T. Dragičević, "Modeling and advanced control of dual-active-bridge dc–dc converters: A review," *IEEE Transactions on Power Electronics*, vol. 37, no. 2, pp. 1524–1547, 2022.

[13] K. S. Narendra and A. M. Annaswamy, *Stable Adaptive Systems*. USA: Prentice-Hall, Inc., 1989.

[14] N. T. Nguyen, *Model-Reference Adaptive Control*. Cham: Springer International Publishing, 2018, pp. 83–123. [Online]. Available: https://doi.org/10.1007/978-3-319-56393-0˙5

[15] P. A. Ioannou and J. Sun, *Robust Adaptive Control*. USA: Prentice-Hall, Inc., 1995.

Authorized licensed use limited to: Missouri University of Science and Technology. Downloaded on February 17,2023 at 18:46:27 UTC from IEEE Xplore. Restrictions apply.

[16] G. Brando, A. Del Pizzo, and S. Meo, "Model-reference adaptive control of a dual active bridge dc-dc converter for aircraft applications," in *2018 International Symposium on Power Electronics, Electrical Drives, Automation and Motion (SPEEDAM)*, 2018, pp. 502–506.

[17] H. Qin and J. W. Kimball, "Generalized average modeling of dual active bridge dc–dc converter," *IEEE Transactions on Power Electronics*, vol. 27, no. 4, pp. 2078–2084, 2012.

Authorized licensed use limited to: Missouri University of Science and Technology. Downloaded on February 17,2023 at 18:46:27 UTC from IEEE Xplore. Restrictions apply.